STEM CELLS®

TISSUE-SPECIFIC STEM CELLS

CRISPR/Cas9-Based Dystrophin Restoration Reveals a Novel Role for Dystrophin in Bioenergetics and Stress Resistance of Muscle Progenitors

POLINA R. MATRE,[a] XIAODONG MU,[a,b] JIANBO WU,[a,c] DELIA DANILA,[d] MARY A. HALL,[a] MIKHAIL G. KOLONIN,[c] RADBOD DARABI,[c] JOHNNY HUARD[a,b,c]

Key Words. CRISPR • Skeletal muscle • Somatic stem cells • Stem/progenitor cell • Stem cells • Tissue-specific stem cells

[a]Department of Orthopaedic Surgery, McGovern Medical School, The University of Texas Health Science Center at Houston, Houston, Texas, USA; [b]Center for Regenerative Sports Medicine, Steadman Philippon Research Institute, Vail, Colorado, USA; [c]Brown Foundation Institute of Molecular Medicine, McGovern Medical School, The University of Texas Health Science Center at Houston, Houston, Texas, USA; [d]Department of Internal Medicine, McGovern Medical School, The University of Texas Health Science Center at Houston, Houston, Texas, USA

Correspondence: Johnny Huard, Ph.D., Center for Regenerative Sports Medicine, Steadman Philippon Research Institute, 181 West Meadow Drive, Suite 1000, Vail, Colorado 81657, USA. Telephone: 970-479-1595; e-mail: jhuard@sprivail.org

Received November 4, 2018; accepted for publication June 26, 2019; first published online October 1, 2019.

http://dx.doi.org/10.1002/stem.3094

ABSTRACT

Although the lack of dystrophin expression in muscle myofibers is the central cause of Duchenne muscular dystrophy (DMD), accumulating evidence suggests that DMD may also be a stem cell disease. Recent studies have revealed dystrophin expression in satellite cells and demonstrated that dystrophin deficiency is directly related to abnormalities in satellite cell polarity, asymmetric division, and epigenetic regulation, thus contributing to the manifestation of the DMD phenotype. Although metabolic and mitochondrial dysfunctions have also been associated with the DMD pathophysiology profile, interestingly, the role of dystrophin with respect to stem cells dysfunction has not been elucidated. In the past few years, editing of the gene that encodes dystrophin has emerged as a promising therapeutic approach for DMD, although the effects of dystrophin restoration in stem cells have not been addressed. Herein, we describe our use of a clustered regularly interspaced short palindromic repeats/Cas9-based system to correct the dystrophin mutation in dystrophic (*mdx*) muscle progenitor cells (MPCs) and show that the expression of dystrophin significantly improved cellular properties of the *mdx* MPCs in vitro. Our findings reveal that dystrophin-restored *mdx* MPCs demonstrated improvements in cell proliferation, differentiation, bioenergetics, and resistance to oxidative and endoplasmic reticulum stress. Furthermore, our in vivo studies demonstrated improved transplantation efficiency of the corrected MPCs in the muscles of *mdx* mice. Our results indicate that changes in cellular energetics and stress resistance via dystrophin restoration enhance muscle progenitor cell function, further validating that dystrophin plays a role in stem cell function and demonstrating the potential for new therapeutic approaches for DMD. STEM CELLS *2019;37:1615–1628*

SIGNIFICANCE STATEMENT

Lack of dystrophin in muscle myofibers is the central cause of Duchenne muscular dystrophy (DMD), the most common inherited muscular dystrophy. Accumulating evidence suggests that DMD may also be a stem cell disease. In this study, the authors restored dystrophin in muscle progenitors using gene editing (clustered regularly interspaced short palindromic repeats/Cas9) and enhanced their function, suggesting a novel role of dystrophin in muscle progenitor and potentially new therapeutic approaches for DMD.

INTRODUCTION

Duchenne muscular dystrophy (DMD) is the most common inherited form of muscular dystrophy. It is an X-linked genetic disorder that primarily affects males and results in the lack of expression of dystrophin, a structural myofiber sarcolemma protein [1]. Dystrophin deficiency leads to progressive weakening and wasting of skeletal, cardiac, and respiratory muscles in DMD patients and, subsequently, premature death [2, 3]. Despite the lack of dystrophin at birth in DMD patients, the histopathological signs of muscle weakness do not typically become apparent until the patient reaches 4–8 years of age, which happens to coincide with depletion of the muscle progenitor cell (MPC) pool [4, 5]. Stem cell-based therapy is a promising treatment for muscular dystrophy due to its capability to restore dystrophin expression and reconstitute the stem cell pool. Over the last 30 years, multiple cell-based therapies have been used in an attempt to deliver the full-length DMD gene via the fusion of donor cells with host myofibers. Although some of these strategies have proceeded to clinical trials, their success has been limited due to

poor cell survival [6–11]. Other current therapies for DMD include gene therapies, such as small molecules that target translation termination caused by nonsense mutations [12, 13] or delivery of truncated DMD genes to dystrophic muscle tissue using viral vectors [14–16]. However, various limitations have hindered the widespread application of gene therapy for DMD [17]. Exon-skipping oligonucleotides have been used successfully in a number of animal models and tested in several clinical trials [18–22]. Although these therapeutic designs are promising, the clinical translation of this work has been limited. Postnatal genome editing via clustered regularly interspaced short palindromic repeats (CRISPR)/CRISPR-associated protein 9 (Cas9) or CRISPR technology has emerged as a promising therapeutic approach for DMD and, in preclinical settings, CRISPR has been shown to restore dystrophin in dystrophic muscle and improve muscle function in *mdx* skeletal muscle [3, 23–25]. Although CRISPR technology represents a valuable therapeutic approach for DMD, it should be noted that most reports on gene editing using viral vectors describe studies performed in young animals and show limited efficiency in aged animals.

The deficiency of dystrophin in myofibers is a generally accepted cause underlying DMD histopathology. However, the muscle wasting observed in DMD patients is a complex process, with repetitive cycles of degeneration followed by regeneration, which consequently exhausts or depletes the functional muscle stem cell pool [4, 5]. Thus, DMD can also be considered a muscle stem cell disease. Indeed, a recent study showed dystrophin expression in satellite cells and revealed a novel role for dystrophin as a key regulator of asymmetric cell division and stem cell function [26, 27]. Dystrophin-null satellite cells exhibit a loss in cell polarity that causes a decrease in the number of myogenic progenitors, resulting in impaired regeneration of dystrophin-null myofibers and progressive muscle loss. In addition, multiple lines of evidence exist that highlight the role of MPC depletion/dysfunction in DMD progression. As mentioned above, the relatively late age of disease manifestation coincides with MPC depletion, despite the lack of dystrophin at birth in DMD patients. In a supporting mouse model, *mdx*/*mTR* mice (dystrophin-deficient with telomere dysfunction, specifically in their MPCs) develop a more severe dystrophic phenotype than that of standard *mdx* mice, which rapidly deteriorates with age due to depletion of MPCs [28]. Similarly, the dystrophin/utrophin double knockout (dKO) mouse, another severely affected model, also features a rapid dystrophic progression that correlates with a defective MPC pool [29, 30]. In addition, a dystrophic muscle microenvironment, such as hypoxia, oxidative and inflammatory stresses, and nutrient deficiency might exacerbate stem cell depletion/dysfunction due to poor stem cell survival under these adverse conditions. Previous studies have indicated that apoptosis is increased in *mdx* mouse muscle and in cultured *mdx* muscle cells [31], and also suggested that cell death in *mdx* muscle may be initiated by apoptosis and followed by necrosis [32–34]. It has been reported that intracellular adenosine triphosphate (ATP) levels, hypoxia, and/or reactive oxygen species (ROS) can dictate whether a cell dies by a primarily necrotic or an apoptotic pathway [35] or direct muscle regeneration [36]. Taken together, these studies suggest that the occurrence of stem cell dysfunction due to the lack of dystrophin is a major contributing factor to the onset of the pathologic features of muscular dystrophy.

In the dystrophic cell, lack of dystrophin leads to complex pathologic changes that drive skeletal muscle weakness, atrophy, and eventually death [2]. The underlying mechanisms are believed to include calcium overload due to cellular and mitochondrial Ca^{2+} entry through tears in dystrophin-deficient sarcolemma or activation of calcium leak channels [37–39], as well as mitochondrial dysfunction due to Ca^{2+} influx through the activation of proteases [40, 41]. However, the effects of dystrophin deficiency on the fundamental aspects of mitochondrial function are not completely understood. Mitochondria play a major role in skeletal muscle energetics due to their primary function of synthesizing ATP by oxidative phosphorylation (oxphos). They also play a pivotal role in muscle cell signaling due to their handling of intramuscular Ca^{2+} and cell death [42]; studies of the role of mitochondria in Ca^{2+} handling and necrotic cell death have provided additional insights into abnormal mitochondrial function in DMD. Mitochondrial dysfunction manifests in both prolonged mitochondrial permeability transition pore opening and in the inhibition of mitochondrial ATP synthesis, which promotes cell death [41, 43, 44]. Myoblasts derived from dystrophic (*mdx*) mice exhibit reduced oxygen consumption, increased mitochondrial membrane potential, and heightened ROS formation [45]. The mitochondrial function may also be impacted by dystrophin deficiency via the disruption of mitochondrial localization, which leads to the uncoupling of oxphos and reducing the maximal rate of ATP synthesis [42]. Several studies have shown an impaired mitochondrial function in the *mdx* mouse model [46], the dKO model [47], and DMD patients [48]. Dystrophin-mediated repair in DMD cardiomyocytes was shown to mitigate the mitochondrial deficiencies [49]. In addition, recent reports provide compelling evidence that mitochondria represent an important drug target for muscular dystrophy [41, 43, 50–52]. Taken together, these studies demonstrate the impairment of mitochondria in DMD myofibers and emphasize the need for mitochondrial studies in dystrophic MPCs. Fascinating new roles for dystrophin in muscle stem cells have recently emerged [26, 27]; however, these studies did not encompass the modulation of mitochondrial and metabolic processes or stress tolerance conferred by dystrophin.

Here, we hypothesized restoration of dystrophin in MPCs would influence their ability to survive, self-renew, and regenerate myofibers within the diseased micromilieu. We, therefore, tested whether dystrophin restoration using CRISPR/Cas9 editing can, in addition to improving the mechanical properties of myofibers, enhance the energetic properties of *mdx* MPCs. We found that dystrophin-restored *mdx* MPCs showed improvements in cell proliferation, differentiation, bioenergetics, and resistance to oxidative and endoplasmic reticulum (ER) stress in vitro. Our in vivo studies revealed improved transplantation efficiency of the dystrophin-restored *mdx* MPCs in the muscles of *mdx* mice. This study provides insight into the mitochondrial and metabolic dysfunction of dystrophic MPCs, which may assist in the identification of new therapeutic approaches for DMD.

Materials and Methods

Cloning of sgRNA and CRISPR/Cas9 System Construction

Four single-guide RNAs (sgRNAs), sgRNA1/2 and sgRNA3/4 (see Supporting Information Table S1), were cloned into a pSpCas9 (BB)-2A-green fluorescent protein (GFP) (PX458) plasmid containing the SpCas9 gene with 2A-enhanced green fluorescent protein (EGFP) and the backbone of the sgRNA (Addgene plasmid #48138). The sequences for sgRNA1/2 have been used

and reported previously [23] The sgRNA3/4 were designed in our lab to target exon 23 using an sgRNA CRISPR design tool (crispr.mit.edu). Cloning of sgRNA was done according to the protocol of Dr. Feng Zhang's lab at the Massachusetts Institute of Technology. In brief, complimentary oligos that contained the appropriate sgRNA sequences and BbsI restriction sites were obtained from Integrated DNA Technologies and annealed to form double-stranded DNA fragments. The resulting fragments and backbone plasmids were digested with BbsI and ligated using a Quick Ligation Kit (New England Biolabs, Ipswich, MA).

MPC Isolation from Skeletal Muscle, Expansion, and Characterization

MPCs were isolated from the skeletal muscle of wild-type (WT) and *mdx* mice using our established, modified preplate technique [53, 54]. The cells were cultured in Dulbecco's modified Eagle's medium (DMEM) supplemented with 20% fetal bovine serum (FBS), 1% penicillin/streptomycin (Invitrogen, Carlsbad, CA), and 0.5% chicken embryo extract (Accurate Chemical Co., Westbury, NY). The cells were cultured in 21% O_2 for normoxia and 1% O_2 for hypoxia conditions. The MPCs underwent myogenic, osteogenic, and chondrogenic differentiation and the degrees of differentiation were measured and compared among the different groups, as previously described [53].

MPC Transfection and Fluorescence-Activated Cell Sorting

JetPRIME reagent (Polyplus-transfection, Illkirch, France) was used to transfect MPCs. The CRISPR/Cas9 system components and GFP reporter was expressed transiently. Two days after transfection, the top 20%–50% of cells having the highest GFP mean fluorescence intensity (MFI) was sorted by Fluorescence-Activated Cell Sorting and expanded in vitro. A loss of GFP reporter was confirmed by fluorescent microscopy.

Immunostaining, Biochemical, and Histochemical Analysis

Immunofluorescence and histological staining were performed as previously described [55]. Gastrocnemius (GC) muscle samples were flash-frozen in liquid nitrogen, 2-methylbutane solution. Frozen sections (10-μm) were fixed with 4% paraformaldehyde for 10 minutes. Sections were washed with phosphate-buffered saline and permeabilized with 0.3% Triton X-100 for 5 minutes, and then blocked with Seablock (Thermo Fisher Scientific, Waltham, MA) for 1 hour at room temperature. Cells or frozen sections were incubated at 4°C overnight with a primary antibody as follows: rabbit antidystrophin (1:200, Abcam, Cambridge, MA), antidystrophin-PE (1:300, SC Biotechnology, Santa Cruz, CA), rabbit anti-laminin 1 antibody (1:100, Abcam, Cambridge, MA), mouse anti-Pax7 (1:100, DSHB, Iowa), or mouse antiembryonic myosin heavy chain (1:50, eMyHC, DSHB, IA). A Mouse on Mouse kit (Vector Laboratories, Burlingame, CA) was used per conditions according to the manufacturer's protocol. Secondary antibodies used were donkey anti-rabbit or anti-mouse Alexa 488- and Alexa 594-conjugated IgG (Invitrogen and Jackson ImmunoResearch, West Grove, PA, respectively) per the manufacturer's instructions. Nuclei were counterstained with 4′,6-diamidino-2-phenylindole (DAPI, 1:1,000, Invitrogen). Image acquisition was performed with a Leica Microsystems Inc. (Buffalo Grove, IL) camera at ×4–40 magnification.

Proliferation, Stress Resistance, and Differentiation Assays

Cell proliferation and viability assays were performed using a CellTiter-Blue Cell Kit (Promega, Madison, WI). Cell cycle analysis was performed using flow cytometry cell cycle analysis with DAPI. The proliferation and differentiation potentials of MPCs were analyzed under 20% O_2 versus 1% O_2, in media containing 400 μM H_2O_2 (oxidative stress) for 3 hours, and in media containing 10 μM eeyarestatin for 6 hours to induce ER stress; and they were cultured in myogenic, osteogenic, and chondrogenic induction media. Chondrogenic (StemPro Chondrogenesis Differentiation Kit, Gibco) and osteogenic (DMEM, 10% FBS, 50 μg/ml ascorbic acid, 10 mM β-glycerophosphate, 10 nM dexamethasone) induction media were used for the respective differentiation assays. Alkaline phosphatase (ALP) staining, computed tomography scanning of pellet cultures, and Alcian blue staining were used to confirm differentiation as described previously [56, 57].

Gene Expression Analysis by Quantitative Real-Time Polymerase Chain Reaction

Total RNA from GC muscle or cells was extracted with TRIzol reagent (Life Technologies, Carlsbad, CA). Specific cDNA was synthesized using the iScript Reverse Transcription Kit (Bio-Rad, Hercules, CA). Quantitative real-time polymerase chain reaction (RT-PCR) was performed using an iCycler Thermal Cycler (Bio-Rad). The gene-specific primer sequences used are listed in Supporting Information Table S2. *Gapdh* and *18s* were used as internal controls to normalize gene expression. All results are expressed as mean ± SEM.

Mitochondrial Effects (JC-1 Staining)

Mitochondrial membrane potential was assessed by flow cytometry using tetraethylbenzimidazolylcarbocyanine iodide (JC-1), a cationic, fluorogenic dye, (Abcam; Cambridge, MA). Treated cells were loaded with JC-1 dye according to the manufacturer's instructions. The JC-1 solution was added at equal volumes and incubated in the dark at 37°C for 15 minutes prior to analysis. For the positive control, MPCs were incubated with uncoupler FCCP (carbonyl cyanide 4-[trifluoromethoxy]phenylhydrazone) before the addition of the JC-1 solution. Monomeric (green) and JC-1-aggregate (red) fluorescence was measured by flow cytometry using green (Ex488/Em530) and red (Ex488/Em585) fluorescence spectra, and analyzed following compensation for spectral overlap.

ATP and Adenosine Diphosphate/ATP Measurements

An adenosine diphosphate (ADP)/ATP ratio bioluminescence assay was used to measure ATP levels and the ADP/ATP ratio (Sigma–Aldrich, St. Louis, MO).

Gas Chromatography–Mass Spectrometry Metabolic Analysis

Gas chromatography–mass spectrometry metabolic analysis (GC–MS) metabolite extraction and analysis were performed at the Metabolomics Core Facility at the University of Utah, as previously described, with minor modifications [55]. Peak intensities of 38 metabolites were obtained for three replicates for each experimental condition.

Western Blotting

Protein extracts from tissues and cultured cells were prepared using a RIPA buffer (Cell Signaling). Protein concentration was determined using the BCA assay (Pierce). Fifty micrograms of total protein per lane were used for differentiated MPCs and muscles from injected adult mice. Samples were denatured at 99°C for 5 minutes before being loaded on to 3%–8% TA precast gels (Invitrogen). Dystrophin and vinculin (loading control) were detected by primary antibodies Mandra1 (1:100, Abcam) and V4505 (1:1,000, Sigma), respectively, followed by horse anti-mouse IgG HRP-conjugated secondary antibody (1:1,000, Cell Signaling Technology). A ChemiDoc imaging system (Bio-Rad) was used to detect chemiluminescence after using a Supersignal West Dura ECL kit (Thermo Fisher). Intensities of dystrophin and vinculin bands were quantified using ImageJ (NIH) and the gel analysis function.

MPC Transplantation

MPC transplantations were carried out as previously described [58]. One- to 3-month-old mice were used for the MPC transplantation experiments (n = 4 per group). Mice were housed and maintained in the barrier facility at the University of Texas Health Science Center at Houston (UTHealth) Center for Laboratory Animal Medicine and Care. All experimental studies were carried out in accordance with protocols approved by the Institutional Animal Care and Use Committee at UTHealth.

Statistical Analysis

Statistical analysis was performed using the statistical software package GraphPad Prism (La Jolla, CA). Statistical differences between groups were determined using an analysis of variance (ANOVA) or a Student's t test. The number of animals used was determined by power analysis based on a two-sample t test or ANOVA using the type I error (α = 0.05) and type II error (β = 0.8). All data were expressed as the mean ± SD or SEM as indicated. A p-value of <.05 was considered statistically significant. For GC–MS metabolic data, statistical analysis was performed using the open source software MetaboAnalyst [59] and GraphPad Prism. The values were averaged, normalized by the sum, log-transformed, and scaled by subtracting the mean and dividing by the SD. The p-values were calculated by two-way ANOVA with Tukey's post hoc test.

Results

Excision of Mutated Exon 23 of the *Dmd* Gene Restores Dystrophin Expression

Adult somatic *mdx* MPCs were isolated using the preplate technique based on their slow adherence to collagen-coated flasks, as described previously [53, 60]. The MPCs are multipotent as they form single-cell clones that have been shown to differentiate into muscle, nerve-related cells, bone, and cartilage [53, 61–65]. We restored dystrophin in the *mdx* MPCs using the CRISPR strategy and following the methodology previously demonstrated as being effective in *mdx* myofibers and satellite cells [3, 23, 24]. We cloned four sgRNAs (Supporting Information Table S1) that target introns next to the mutated exon 23 of the *Dmd* mouse gene. All constructs were tested for their ability to produce double-stranded genomic DNA breaks in 3 T3 mouse fibroblasts, both alone by the Surveyor assay and in pairs for deletion of exon 23 by genomic PCR (Fig. 1B and Supporting Information Fig. S1A–S1C). The *mdx* MPCs were transiently transfected with the CRISPR/Cas9 system constructs that express SpCas9 nuclease, specific sgRNA, and GFP) as a reporter. The tested sgRNA pairs produced the anticipated deletion with comparable efficiencies. Thus, for further analysis, we selected edited MPCs that were corrected by the pair of sgRNAs described previously [23], sgRNA1 and sgRNA2 (Supporting Information Table S1). Off-target analysis has previously been performed for these sgRNAs, and no significant off-target mutations were reported [23]. We showed that similar to previously published results [3, 23, 24], the selected sgRNA pair efficiently guided the excision of mutated exon 23 in *mdx* MPCs (Fig. 1). After sorting MPCs for GFP, we confirmed the efficacy and accuracy of the exon 23 deletion of the *Dmd* gene using genomic PCR analysis with primers flanking the sgRNA binding sites (Fig. 1B). The amplicon was also sequenced to demonstrate the irreversible genomic correction and the site of non-homologous end joining (Supporting Information Fig. S2). We induced differentiation of the control and corrected *mdx* MPCs into myotubes, which are known to express dystrophin at high levels, and tested the edits at the transcriptional level by quantitative RT-PCR. Our results showed that ~65% of the transcripts had exon 23 excised. Control RT-PCR using primers amplifying a nonmutated region of exon 45 showed the *Dmd* transcript at similar levels in the *mdx* and dystrophin-restored myotubes (Fig. 1C). The transcription levels of the myogenic regulatory factor Myf5 were used as a positive control for myogenesis (Fig. 1C). Furthermore, to determine whether genomic deletion led to the restoration of the dystrophin protein expression, we induced myogenic differentiation of the edited MPCs and measured dystrophin expression. Western blot analysis revealed expression of the restored dystrophin protein, which migrated at ~430 kDa (as expected; Fig. 1D). Immunostaining also confirmed comparable dystrophin expression in WT and dystrophin-restored *mdx* myotubes (Fig. 1E). The genomic editing of MPCs using sgRNA3and sgRNA4 produced similar results (Supporting Information Fig. S2).

CRISPR/Cas9-Mediated Dystrophin Restoration Improves Multilineage MPC Differentiation

We sought to evaluate how dystrophin restoration affects the multilineage differentiation of *mdx* MPCs. We performed semi-quantitative RT-PCR on modified and control MPCs after 24-hour cultivation in myogenic differentiation media. Analysis of gene expression revealed increased mRNA levels in dystrophin-restored MPCs for multiple myogenesis markers, such as *Pax3* (p = .017), *Pax7* (p = .02), and *Myf5* (p = .02), indicating that the myogenic differentiation potential was increased after dystrophin restoration (Fig. 2A). *MyoD* and *Myog*, late markers of myogenesis, were not significantly upregulated Fig. 2A). In addition, we evaluated the chondrogenic and osteogenic potential of dystrophin-restored MPCs. After *mdx* and dystrophin-restored *mdx* MPCs were cultured in chondrogenic and osteogenic differentiation induction media for 3 days, both chondrogenesis and osteogenesis were increased in dystrophin-restored *mdx* MPCs when compared with unmodified *mdx* MPCs. Gene expression analysis revealed increased mRNA levels for multiple chondrogenic markers, such as aggrecan (*Acan*, p = .038), collagen type II α 1 (*Col2a1*, p = .001), *Sox5* (p = .0175), and *Sox9* (p = .0007), and osteogenic markers, such as *Alp* (p = .01), collagen type I α 1 (*Col1a1*,

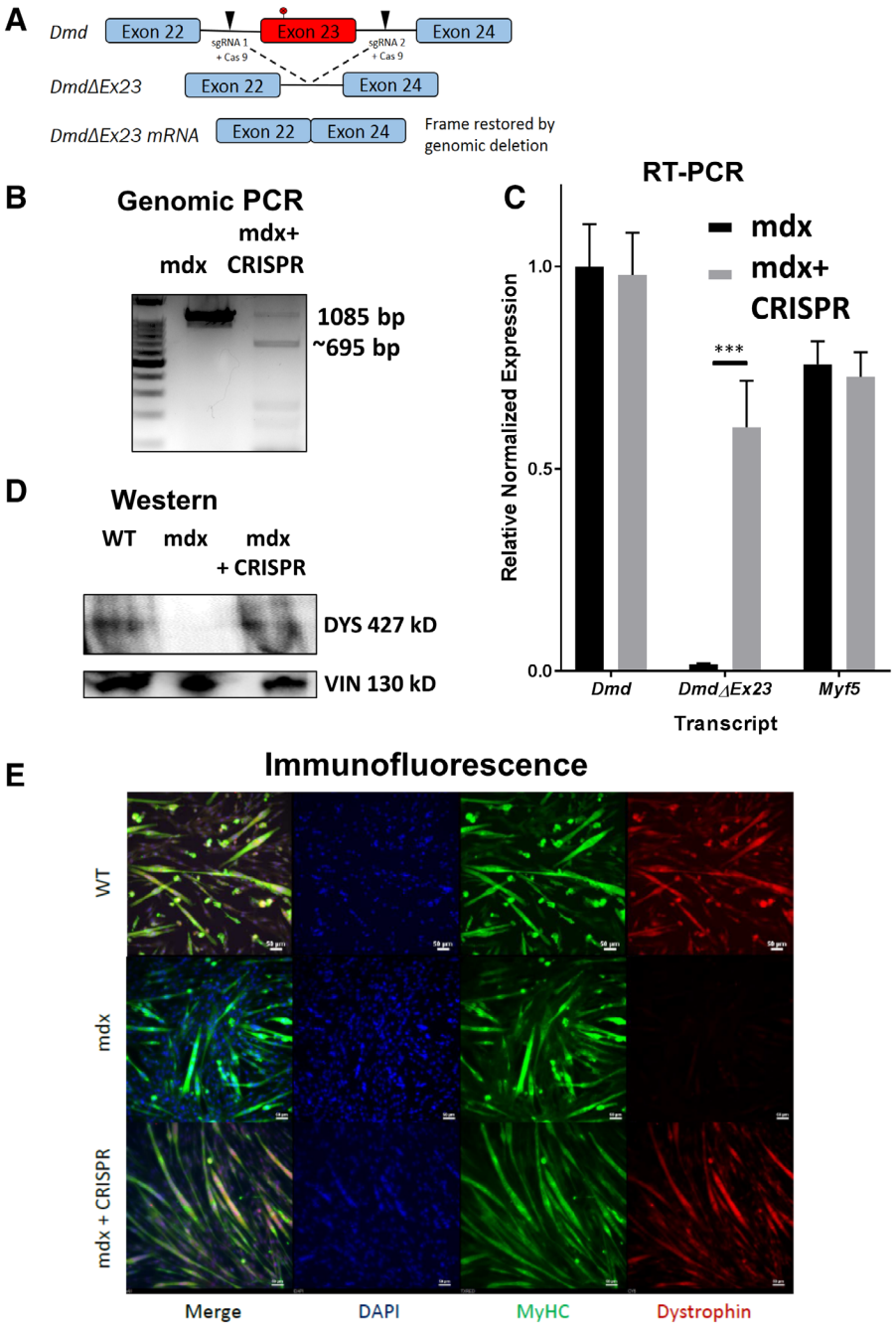

Figure 1. Dystrophin restoration in *mdx* muscle progenitor cells (MPCs) using clustered regularly interspaced short palindromic repeats (CRISPR)/Cas9. **(A):** Schematic representation of the strategy used to restore in-frame dystrophin expression in the *mdx* genomic locus using CRISPR/Cas9-mediated editing. **(B):** Detection of exon 23 (ΔEx23) excision by genomic polymerase chain reaction (PCR); ΔEx23 *Dmd*: 410 bp; unedited PCR product of the *mdx* genomic DNA: 1085 bp. **(C):** Real-time (RT)-PCR of extracts from *mdx* and *mdx* + CRISPR MPCs (differentiated into myotubes) using primers detecting the unmodified *Dmd* and ΔEx23 *Dmd* transcript; Myf5 used as control; ***, $p < .001$. **(D):** Western blot to detect dystrophin protein in myotubes from wild-type (WT), dystrophin-restored *mdx*, and unedited *mdx* MPCs. **(E):** Immunofluorescence microscopy for detection of dystrophin in myotubes derived from WT, *mdx*, and dystrophin-restored *mdx* MPCs (mdx + CRISPR); DAPI (nuclei, blue), myosin heavy chain (MyHC, green), dystrophin (red); scale bar: 50 μm.

$p = .03$), *Col2a1* ($p = .0013$), Osterix (*OSX*, $p = .02$), osteocalcin (*OC*, $p = .002$), runt-related transcription factor 2 (*Runx2*, $p = .0005$), and sirtuin 1 (*Sirt1*, $p = .002$). We further confirmed our results using in vitro staining for myosin heavy chain (MyHC) and ALP as myogenic and osteogenic markers, respectively. Immunofluorescence microscopy scoring showed a 10% increase in the fusion of myotubes with dystrophin-restored *mdx* MPCs compared with unmodified *mdx* MPCs after a 5-day myogenic induction in vitro (Fig. 2B). ALP staining following a 5-day osteogenic induction in vitro confirmed a significant increase in osteogenic differentiation (Fig. 2C). We have confirmed the enhanced differentiation potential using osteogenic (Fig. 2D) and chondrogenic (Fig. 2E) pellet cultures. Together, these results indicate that dystrophin-restored *mdx* MPCs via CRISPR/Cas9

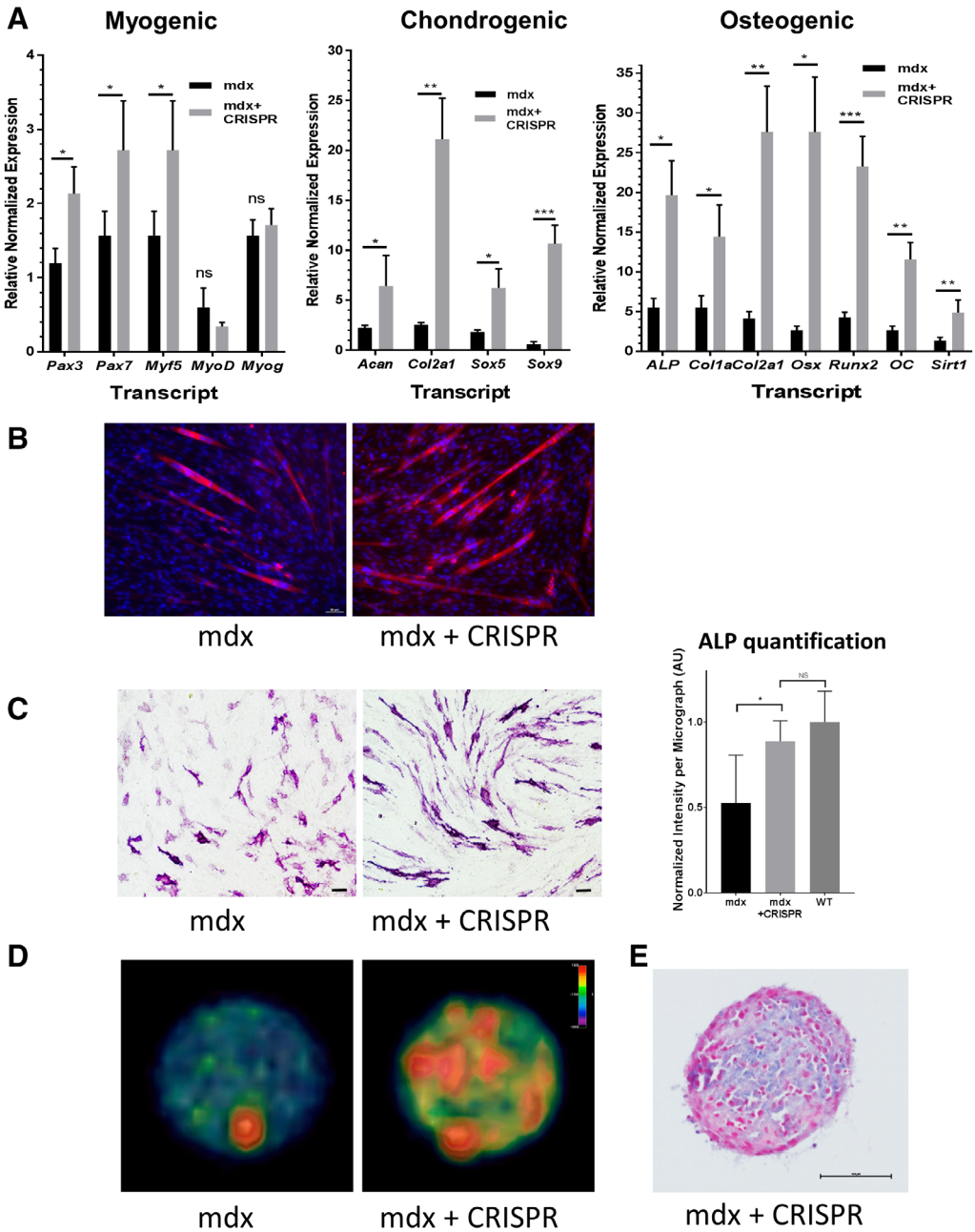

Figure 2. Clustered regularly interspaced short palindromic repeats (CRISPR)/Cas9-modified *mdx* muscle progenitor cells (MPCs) showed improvement in differentiation potential when compared with control, unmodified *mdx* MPCs. **(A):** Quantitative real-time polymerase chain reaction (RT-PCR) results show increases in expression of myogenic, chondrogenic, and osteogenic markers in dystrophin-restored MPCs when compared with control *mdx* MPCs. Cells were cultured for 1–3 days in the corresponding induction media; *, $p < .05$; **, $p < .01$; ***, $p < .001$. **(B):** in vitro myogenesis for dystrophin-restored MPCs and *mdx* control MPCs; myosin heavy chain (MyHC, red), DAPI (nuclei, blue). **(C):** Alkaline phosphatase (ALP) staining for osteogenic differentiation. Quantification of ALP staining intensity shows increased intensity for dystrophin-restored MPCs relative to *mdx* MPCs (right panel); *, $p < .0214$. **(D):** CT scan of osteogenic pellet culture shows improved calcification for dystrophin-restored MPCs when compared with control *mdx* MPCs. **(E):** Alcian blue staining of chondrogenic pellet culture shows improved chondrogenic differentiation and pellet formation for dystrophin-restored MPCs when compared with control *mdx* MPCs that do not grow and form the pellet (not shown). MPCs were cultured for 4 weeks in chondrogenic media. Scale bar: 100 μm.

editing have improved multipotent differentiation potentials for myogenic, osteogenic, and chondrogenic lineages.

Increased Stress Resistance and Proliferation of Dystrophin-Restored *mdx* MPCs

To further understand the changes associated with dystrophin restoration in *mdx* MPCs, we investigated their proliferative and stress resistance properties and compared the results with those of unmodified (control) *mdx* MPCs. In particular, we were interested in characterizing cell survival and proliferation under stress conditions that are typical of dystrophic muscle, such as conditions of low oxygen, oxidative stress, and protein synthesis stress. The cell viability assay showed no changes in growth under normal growth conditions with 21% oxygen. Cell

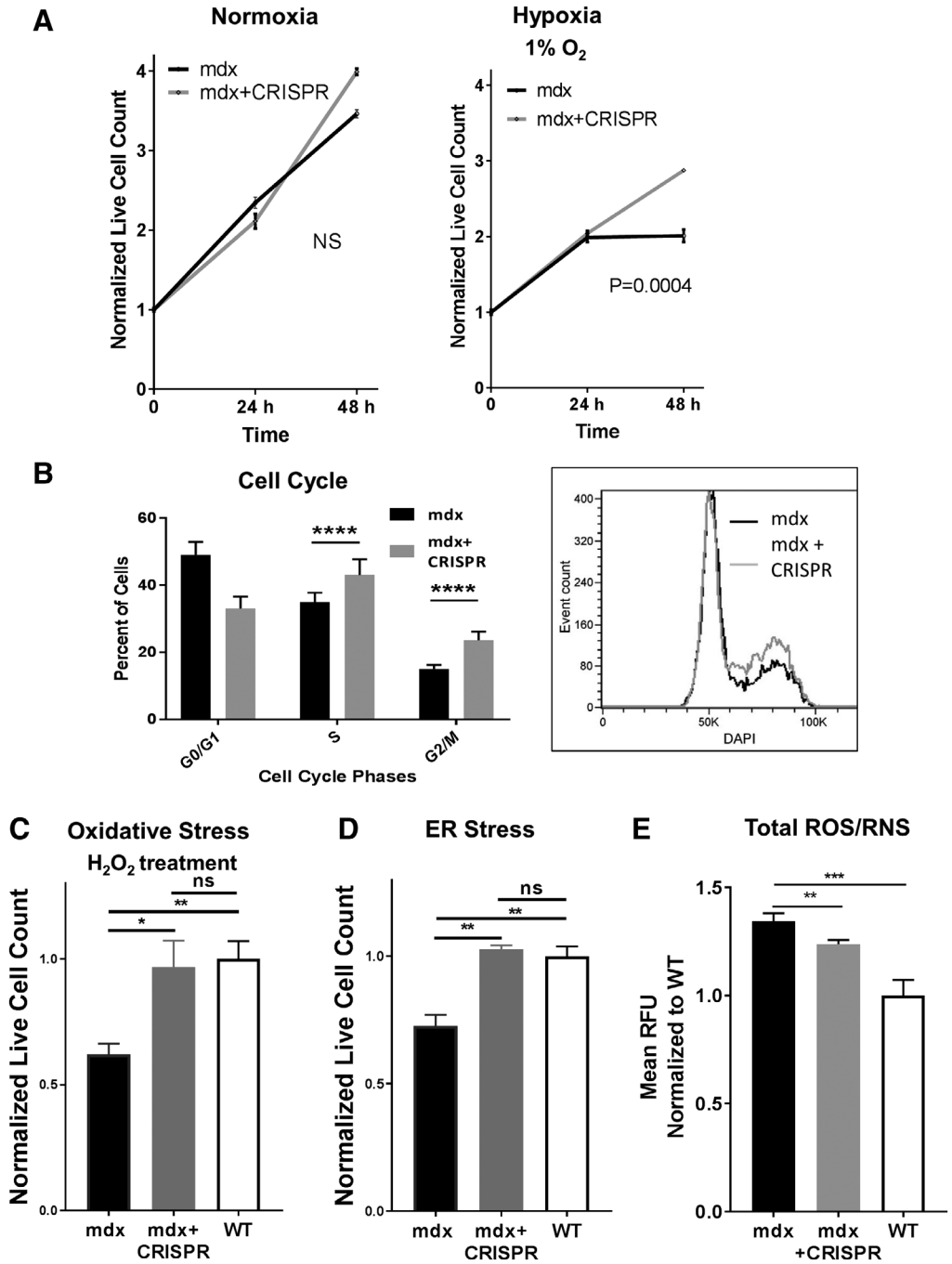

Figure 3. Restoration of dystrophin in *mdx* muscle progenitor cells (MPCs) improved cellular growth and proliferation. **(A):** Corrected *mdx* + clustered regularly interspaced short palindromic repeats (CRISPR) MPCs showed improved growth by 43% after 48 hours of hypoxia (1% O_2). Under normoxic conditions (21% O_2), live cell counts were slightly improved for *mdx* + CRISPR cells; however, the differences were not statistically significant. The cell number was normalized to the zero time point and is shown as mean ± SEM; ****, $p = .0004$; *t* test for the area under the curve. **(B):** Flow cytometry cell cycle analysis showed small increases in percentages for both S and G2/M phase cells for *mdx* + CRISPR when compared with *mdx* control MPCs, indicating an increase in the proliferation rate (left panel); ****, $p < .0001$. Representative overlay of DAPI-stained *mdx* control and dystrophin-restored *mdx* + CRISPR MPCs in a flow cytometric analysis histogram (right panel). **(C–E):** Restoration of dystrophin in dystrophic MPCs improved cellular growth under stressors and repressed oxidative stress. Cell viability assay on wild-type (WT), *mdx* control, and *mdx* + CRISPR MPCs after (C) oxidative stress and (D) endoplasmic reticulum (ER) stress treatment. Cell counts were normalized to respective untreated control and WT cells, and the results are shown as mean ± SEM; *, $p < .05$; **, $p < .01$. (E): Dystrophin correction decreased reactive oxygen species (ROS)/RNS production. Higher ROS accumulation (ROS/RNS) was observed in *mdx* cells relative to WT cells, which was decreased by approximately 10% in corrected *mdx* + CRISPR cells; **, $p = .0019$.

growth for dystrophin-restored MPCs was also improved by roughly 40% under hypoxic conditions (O_2 1%), when compared with control *mdx* MPCs (Fig. 3A). In addition, following exposure to oxidative (hydrogen peroxide, H_2O_2) and ER stress in dystrophin-restored *mdx* MPCs, the viability was higher than that of unmodified *mdx* MPCs by 36% ($p = .02$) (Fig. 3C) and 28%

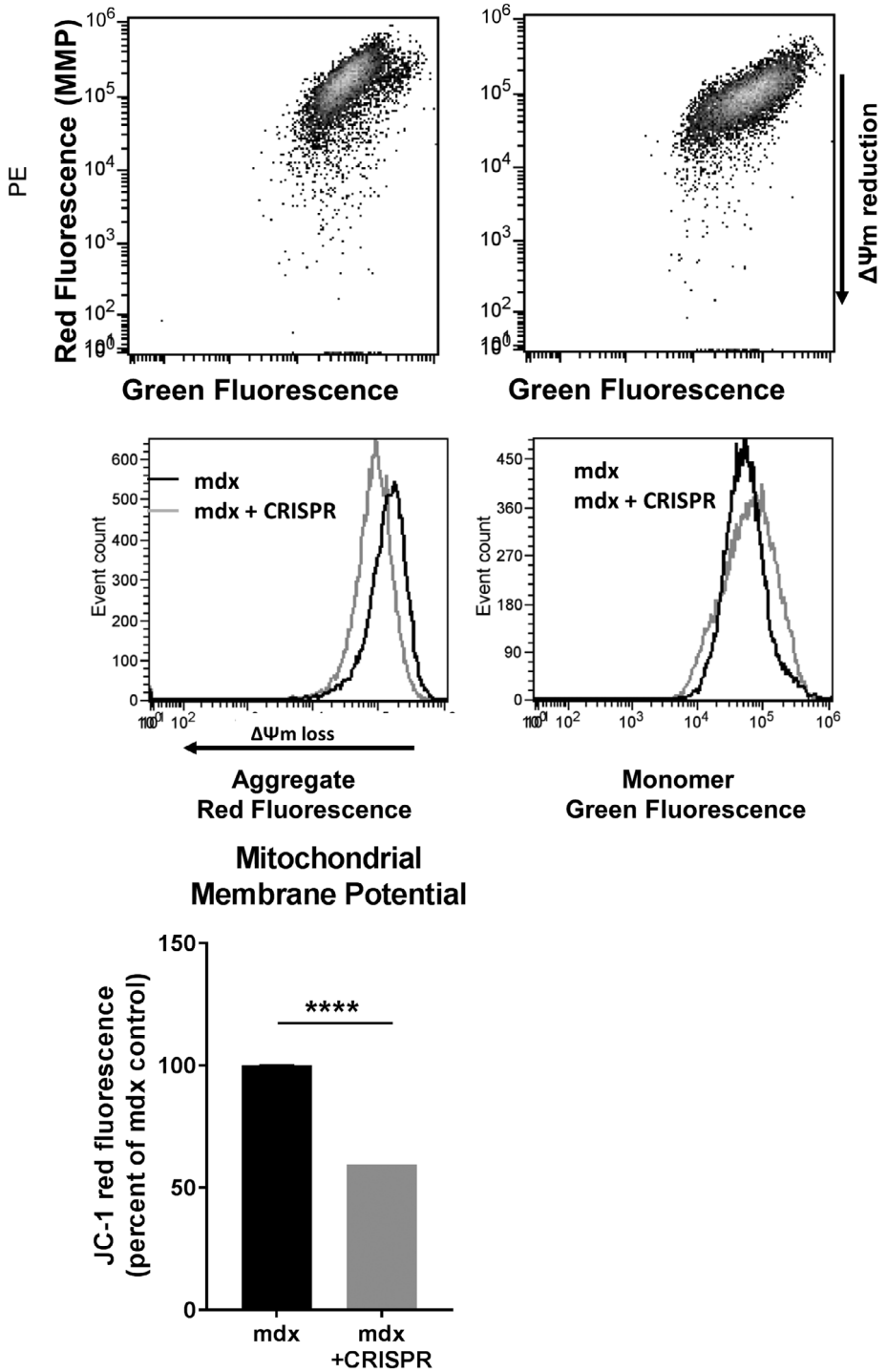

Figure 4. Dystrophin restoration repressed oxidative stress in *mdx* muscle progenitor cells (MPCs). Analysis of mitochondrial membrane potential (ΔΨm) measured by flow cytometry (JC-1 aggregate emits red fluorescence) showed notable decreases in ΔΨm (∼40%, ****, $p < .0001$) for dystrophin-restored (*mdx* + clustered regularly interspaced short palindromic repeats [CRISPR]) MPCs compared with control *mdx* MPCs. JC-1 monomer mean fluorescence intensity (MFI) measurements (emits green fluorescence) were not significantly different for *mdx* versus *mdx* + CRISPR MPCs. The mean fluorescence intensity (MFI) of samples treated with a known uncoupler (FCCP) was used as a positive control for ΔΨm loss.

($p = .005$; Fig. 3D), respectively, indicating that dystrophin restoration improves *mdx* MPCs' resistance to stress (Fig. 3C, 3D). Notably, dystrophin-restored *mdx* and WT MPCs showed no statistically significant differences in viability after the stress treatments (Fig. 3C, 3D). Flow cytometry cell cycle analysis showed an increased percentage of G2/M cells in dystrophin-restored *mdx* MPCs compared with control *mdx* MPCs, indicating faster cell growth and a higher rate of proliferation (Fig. 3B).

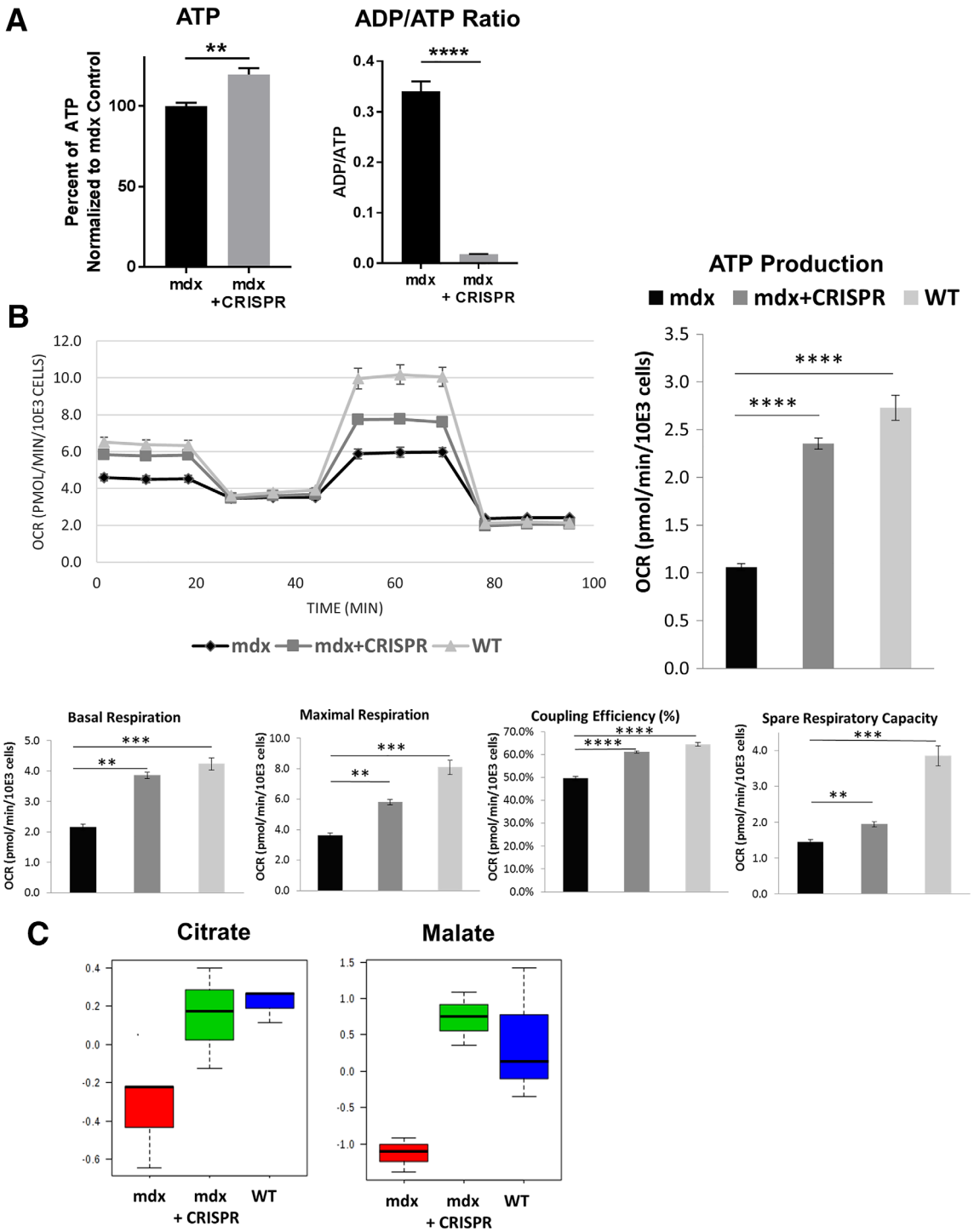

Figure 5. Dystrophin restoration improved mitochondrial function in *mdx* muscle progenitor cells (MPCs). **(A):** A bioluminescence assay was used to measure adenosine diphosphate (ADP) and adenosine triphosphate (ATP) levels (relative light units per well) in *mdx* and *mdx* + clustered regularly interspaced short palindromic repeats (CRISPR) cells. Intracellular ATP content was increased by 20% in dystrophin-restored cells relative to *mdx* MPCs; **, $p < .01$. The ADP/ATP ratio was significantly lower in *mdx* + CRISPR cells, indicating lower apoptosis; ****, $p < .0001$. **(B):** To characterize the effects of dystrophin restoration on respiration, oxygen consumption rate (OCR) was measured using a Seahorse Bioscience XF24 extracellular flux analyzer. Dystrophin restoration increased basal OCR, ATP production, and maximal respiratory capacity in MPCs. Spare respiratory capacity and mitochondrial coupling were improved as well. Four replicate wells ($50–60 \times 10^5$ cells per well) were analyzed. OCR values were normalized to the number of cells per well. **(C):** Gas chromatography–mass spectrometry-based metabolomics analysis of *mdx*, dystrophin-corrected, and wild-type MPCs. Semiquantitative analysis revealed that levels of the tricarboxylic acid cycle intermediates citrate ($p = .03$) and malate ($p = .0069$) were increased in dystrophin-restored MPCs. Peak intensities of 38 metabolites were obtained from each of three replicates per metabolite. The values were averaged for each metabolite, normalized by the sum and log-transformed, and then scaled by subtracting the mean and dividing by the SD. The *p*-values were calculated by one-way analysis of variance with Tukey's post hoc test; SD is shown with bars.

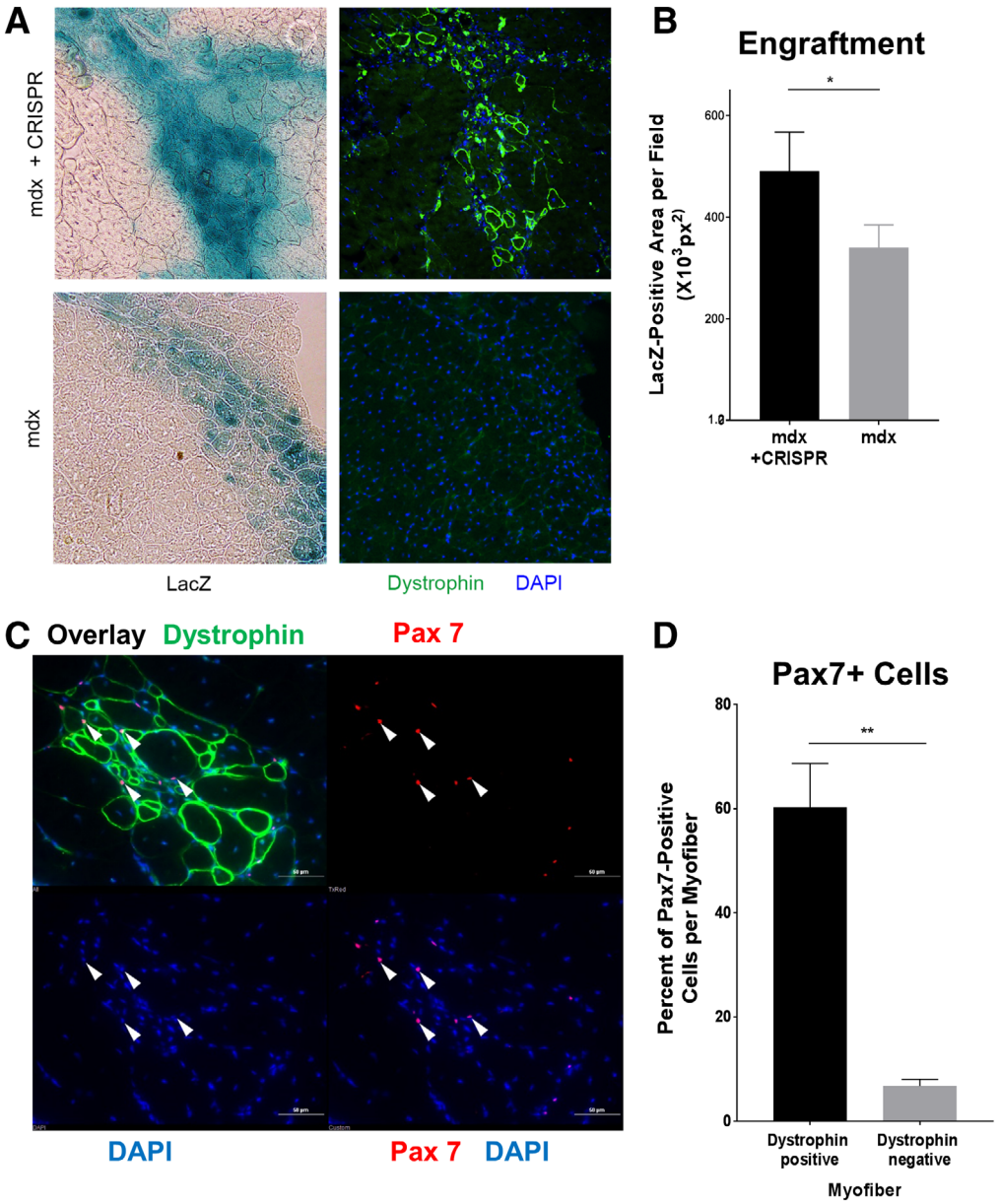

Figure 6. Survival and engraftment of dystrophin-restored *mdx* muscle progenitor cells (MPCs) in *mdx* skeletal muscle. **(A):** Immunofluorescent staining of gastrocnemius (GC) muscle shows dystrophin expression in LacZ-positive myofibers (labeled *mdx* + clustered regularly interspaced short palindromic repeats [CRISPR]) after transplantation. Right top panel shows dystrophin-positive myofibers labeled green and DAPI-positive nuclei labeled blue; left top panel shows LacZ-positive myofibers labeled blue. No dystrophin expression was observed in myofibers derived from unmodified LacZ-labeled *mdx* MPCs (labeled *mdx*, bottom panels). **(B):** Histomorphometric analysis based on the LacZ-positive area of grafts showed greater cell engraftment for dystrophin-restored MPCs (labeled *mdx* + CRISPR) than for *mdx* MPCs. GC muscle cross-sections (n = 10) of mice (n = 4 per group) that were sacrificed 4 weeks after intramuscular injection (1×10^6 cells per injection) were analyzed by phase-contrast microscopy. And the results are shown as mean ± SEM; *, $p < .05$. **(C):** Pax 7+ MPCs were expanded at the graft site. Immunofluorescent staining of GC muscle shows dystrophin protein expression in newly regenerated myofibers (green) and Pax7+ MPCs (red) at the site of engraftment. **(D):** Numbers of Pax7+ cells per dystrophin-positive myofiber were increased significantly (p = .0036) compared with numbers of Pax7+ cells in dystrophin-negative myofibers, and the results are shown as mean ± SEM; **, $p < .01$.

Improved Mitochondria Function and Repressed Oxidative Stress in Dystrophin-Restored *mdx* MPCs

The dystrophic microenvironment is characterized by a high level of oxidative stress that is known to cause damage to mitochondria due to ROS, thus disrupting overall energy generation in the cell. In addition, dysregulated mitochondrial respiration might contribute to higher levels of ROS as well as promote further damage in the dystrophic cell. To investigate whether CRISPR/Cas9-mediated gene editing can boost the cell survival properties of *mdx* MPCs in the dystrophic microenvironment, we measured the ROS levels in dystrophin-restored *mdx* MPCs, *mdx* MPCs, and WT control MPCs. The *mdx* cells had significantly higher levels of total reactive oxygen/nitrogen species (ROS/RNS) than did WT MPCs (p = .0001, Fig. 3E). However, the observed higher level of

ROS/RNS production by *mdx* MPCs was decreased by ~10% in dystrophin-restored *mdx* MPCs (p = .0019, Fig. 3E). Although, the levels of intracellular H_2O_2, a type of ROS, were not significantly different in *mdx* MPCs compared with dystrophin-restored *mdx* MPCs (data not shown).

To further examine mitochondrial function, we assessed the transmembrane potential ($\Delta\Psi$m). Mitochondrial $\Delta\Psi$m is critical for maintaining the physiological function of the respiratory chain necessary to generate ATP. In *mdx* myoblasts, the observed mitochondrial $\Delta\Psi$m is known to be adversely elevated when compared with WT myoblasts [45]. Analysis of mitochondrial $\Delta\Psi$m measured by flow cytometry (aggregate red fluorescence) showed a notable decrease in dystrophin-restored *mdx* MPCs compared with control *mdx* MPCs, with a substantial decrease in MFI by ~40% compared with control *mdx* MPCs. The MFI of samples treated with a known uncoupling agent, FCCP (carbonyl cyanide-p-trifluoromethoxyphenylhydrazone), was used as a positive control for $\Delta\Psi$m loss (Fig. 4). In summary, we observed a significant normalization of mitochondrial $\Delta\Psi$m in *mdx* MPCs after dystrophin restoration.

To corroborate the improvements in mitochondrial function after dystrophin restoration in *mdx* MPCs, we measured ADP and ATP levels in control *mdx* and dystrophin-restored *mdx* MPCs. First, we used a bioluminescence assay and showed a 20% increase in ATP levels in dystrophin-restored MPCs (p = .0048). Control *mdx* MPCs had a dramatically higher ADP/ATP ratio, which may be indicative of increased levels of apoptosis (Fig. 5A). Lower ATP levels in *mdx* MPCs reinforce the idea that the lack of dystrophin compromises overall energy production; our results support this and indicate that dystrophin restoration reverses the effect.

Based on the effects of dystrophin restoration on bioenergetic characteristics, such as $\Delta\Psi$m, ROS and ATP production, and changes in cellular growth, we further investigated modulations of mitochondrial function, particularly mitochondrial respiration (Fig. 5B). We evaluated the oxygen consumption rate (OCR), a measure of overall mitochondrial respiration, and characterized the effect of dystrophin restoration on OCR. We observed that dystrophin restoration caused a significant increase in basal mitochondrial respiration (p = .0012). In addition, ATP production (p < .0001; which was calculated as the difference between the basal level and OCR after oligomycin treatment) and maximal respiratory capacity (p = .0013; which was calculated after FCCP was added) were restored to levels closer to those measured in WT control MPCs. The spare respiratory capacity, calculated as the difference between basal and maximal respiration, was improved (p = .0044), along with the mitochondrial coupling efficiency (p < .0001) in the dystrophin-corrected *mdx* MPCs. (Fig. 5B). To investigate whether restoration of dystrophin in MPCs can improve bioenergetics properties in differentiated MPCs (myotubes), we measured OCR in differentiated myotubes (Supporting Information Fig. S3) and observed similar results as mdx undifferentiated MPCs (Fig. 5).

To corroborate our findings, we performed GC–MS-based metabolomics analysis by collecting peak intensities of 38 metabolites from three replicates of cultured *mdx*, dystrophin-restored, and WT MPCs. The semiquantitative analysis showed that levels of Krebs cycle intermediates, such as citrate (p = .0124) and malate (p = .0328), were significantly decreased in *mdx* MPCs compared with the WT control cells, which indicates lower levels of tricarboxylic acid (TCA) cycle activity. Dystrophin restoration appeared to repair the TCA cycle and restore levels of these important Krebs cycle metabolites, as levels of citrate (p = .03) and malate (p = .0069) were increased in dystrophin-restored *mdx* MPCs compared with WT MPCs (Fig. 5C). Collectively, our data show a significant improvement in mitochondrial function associated with dystrophin restoration in *mdx* MPCs, as determined by metabolic measurements.

Improved Engraftment of Dystrophin-Restored *mdx* MPCs

Finally, we evaluated the regenerative potential of gene-corrected *mdx* MPCs in vivo. Either the corrected or uncorrected *mdx* MPCs, each labeled with a Lenti-LacZ marker, were intramuscularly injected into the GC muscle. The GC muscles were harvested 3 weeks following transplantation, and frozen sections were evaluated for engraftment using beta-galactosidase and anti-dystrophin antibody staining. Although no dystrophin expression was detected in control-injected muscles (*mdx*), except for occasional revertant fibers, muscles that had been injected with CRISPR/Cas9-corrected cells (*mdx* + CRISPR) generated engrafted areas with dystrophin-positive myofibers (Fig. 6A). Histomorphometric analysis based on the LacZ-positive area of grafts confirmed the significantly greater cell engraftment for dystrophin-restored *mdx* MPCs (Fig. 6B). The numbers of Pax7+ satellite cells were dramatically increased proximal to the modified dystrophin-positive myofibers relative to *mdx* control myofibers (0.6 Pax7+ cells per myofiber vs. 0.06 in controls; p = .0036). These data (Fig. 6C, 6D and Supporting Information Fig. S4) indicate that gene-corrected *mdx* MPCs transplanted into *mdx* skeletal muscle may contribute to satellite cell compartment directly or indirectly.

Discussion

Myofiber dystrophin deficiency is generally accepted as a cause of DMD histopathology [2]. The muscle wasting process observed in DMD patients is complex; in addition to causing muscle fragility, DMD is also a muscle stem cell disease. A recent study showed dystrophin expression in satellite cells and revealed a novel role of dystrophin in stem cell function [26, 27]. Herein, we provide additional evidence and fresh insight into the autonomous defects of dystrophic stem cells in muscular dystrophy. Our findings provide further details and previously undescribed effects of dystrophin deficiency in MPCs with respect to bioenergetics and stress resistance. Here, we demonstrate improvements in dystrophin-restored *mdx* MPC characteristics, such as cell proliferation, differentiation, and stress resistance in vitro, as well as enhanced survival of these modified MPCs upon transplantation in vivo and their ability to regenerate dystrophic muscle. To our knowledge, the only published study of dystrophin restoration in muscle stem cells derived from an *mdx* mouse model showed successful restoration, but did not describe the effects of such restoration on the intrinsic properties of the stem cells [38]. It has been reported that, for human DMD cardiomyocytes, some of the dystrophin corrections by CRISPR-Cpf1 also led to improved mitochondrial function [49]. Further research is necessary to determine if the approach for dystrophin restoration used in the current study will confer similar benefits to human MPC properties.

Metabolic dysregulation and mitochondrial dysfunction are important components of the DMD phenotype. However, previous studies have primarily focused on skeletal muscle as a whole,

or only on myoblasts or myofibers at the cellular level [47]. Mitochondrial dysfunction has been attributed to several mechanisms, such as mislocalization of mitochondria within muscle fibers and the functional aberration of mitochondria due to calcium overload [46]. Even though our in vitro studies revealed no obvious changes in mitochondria localization between the *mdx*, dystrophin-restored, and WT MPCs, future studies in vivo are necessary to confirm the unchanged mitochondria localization in dystrophin-restored MPCs. Interestingly, our in vitro studies clearly demonstrated improvement in mitochondrial function following dystrophin restoration, such as increased ATP production and both basal and maximal OCR, as well as higher concentrations of TCA cycle metabolites.

We demonstrated that dystrophin-restored MPCs exhibit an improved growth curve, enhanced proliferation, and lower levels of cell death, especially when cultivated under stressful conditions. The improvement in growth under conditions of stress, such as oxidative and ER stress, underlines the importance of dystrophin for MPC survival and self-renewal upon transplantation to dystrophic muscle. Dystrophic muscle is characterized by a micromilieu with high levels of inflammation and oxidative stress. The gene-edited MPCs appeared to possess an enhanced capability for handling ROS as well. One might speculate that dystrophin may be involved in the regulation of mitochondrial function through improved calcium channeling by mitochondria. This could be the result of the restored mitochondrial capacity to buffer Ca + or a reduction in the activity of Ca^{+}-dependent proteases, which are analogous to mechanisms proposed in prior studies [59]. However, in satellite cells, dystrophin does not function in its typical fashion as a stabilization protein on the intracellular side of the cell membrane. Notably, the dystrophin-glycoprotein complex of satellite cells has been demonstrated to have only basal location [26]. Thus, the underlying mechanisms by which dystrophin impacts mitochondrial processes are beyond the scope of this work and need to be elucidated. Nevertheless, our in vivo results provide strong evidence to support our in vitro findings—that is, restoring dystrophin in MPCs improves their ability to survive, self-renew, and regenerate myofibers within the diseased micromilieu.

Conclusion

In summary, the current study provides proof-of-concept evidence supporting the efficacy of ex vivo genome editing to correct detrimental mutations in dystrophic MPCs and fosters the apparent need for further investigation of new approaches for stem cell therapy. Despite being a heavily explored approach, stem cell therapy has failed during clinical translation due to many limitations, including poor cell survival. Progress in this direction will have a direct impact on improving current clinical therapeutic modalities and outcomes for DMD patients, potentially by adding novel dystrophin restoration methods using CRISPR/Cas9 to therapeutic approaches to reduce stem cell depletion. The demonstrated improvements in survival, proliferation, and differentiation of dystrophin-restored *mdx* MPCs are remarkable and should have significant impact not only on the development of new therapies for the treatment of DMD, but also on our efforts to further understand of the role of dystrophin in muscle stem cells and stem cell biology.

Acknowledgments

This work was supported, in part, by startup funding from the University of Texas Health Science Center at Houston, Houston, TX, and by a philanthropic gift from the Shear Family Foundation to the Steadman Philippon Research Institute, Vail, CO. The authors also thank Dr. Aiping Lu, Dr. Chieh Tseng, and Ms. Haiying Pan for scientific expertise and technical support.

Author Contributions

P.R.M.: study concept and experimental design, and contributed experiments, data analysis and interpretation, writing of the manuscript, and review of the manuscript and concur with the content; X.M., J.W., D.D.: experiments, data analysis, scientific consultation, and review of the manuscript and concur with the content; M.A.H.: manuscript writing, editing, scientific consultation, and review of the manuscript and concur with the content; M.G.K., R.D., J.H.: experimental design, scientific consultation, and review of the manuscript and concur with the content.

Disclosure of Potential Conflicts of Interest

The authors indicated no potential conflicts of interest.

Data Availability Statement

The data that support the findings of this study are available from the corresponding author upon reasonable request.

References

1 Bakay M, Zhao P, Chen J et al. A web-accessible complete transcriptome of normal human and DMD muscle. Neuromusc Disord 2002;12:S125–S141.

2 Hoffman EP, Brown RH Jr, Kunkel LM. Dystrophin: The protein product of the Duchenne muscular dystrophy locus. Cell 1987;51:919–928.

3 Tabebordbar M, Zhu K, Cheng JK et al. In vivo gene editing in dystrophic mouse muscle and muscle stem cells. Science 2016; 351:407–411.

4 Blau HM, Webster C, Pavlath GK. Defective myoblasts identified in Duchenne muscular dystrophy. Proc Natl Acad Sci USA 1983;80: 4856–4860.

5 Zhu CH, Mouly V, Cooper RN et al. Cellular senescence in human myoblasts is overcome by human telomerase reverse transcriptase and cyclin-dependent kinase 4: Consequences in aging muscle and therapeutic strategies for muscular dystrophies. Aging Cell 2007;6: 515–523.

6 Law PK, Goodwin TG, Fang Q et al. Feasibility, safety, and efficacy of myoblast transfer therapy on Duchenne muscular dystrophy boys. Cell Transplant 1992;1:235–244.

7 Gussoni E, Pavlath GK, Lanctot AM et al. Normal dystrophin transcripts detected in Duchenne muscular dystrophy patients after myoblast transplantation. Nature 1992;356: 435–438.

8 Mendell JR, Kissel JT, Amato AA et al. Myoblast transfer in the treatment of Duchenne's muscular dystrophy. N Engl J Med 1995;333: 832–838.

9 Palmieri B, Tremblay JP, Daniele L. Past, present and future of myoblast transplantation

in the treatment of Duchenne muscular dystrophy. Pediatr Transplant 2010;14:813–819.
10 Farini A, Razini P, Erratico S et al. Cell based therapy for Duchenne muscular dystrophy. J Cell Physiol 2009;221:526–534.
11 Farini A, Villa C, Manescu A et al. Novel insight into stem cell trafficking in dystrophic muscles. Int J Nanomed 2012;7:3059–3067.
12 Welch EM, Barton ER, Zhuo J et al. PTC124 targets genetic disorders caused by nonsense mutations. Nature 2007;447:87–91.
13 Gonzalez-Hilarion S, Beghyn T, Jia J et al. Rescue of nonsense mutations by amlexanox in human cells. Orphanet J Rare Dis 2012; 7:58.
14 Wang B, Li J, Xiao X. Adeno-associated virus vector carrying human minidystrophin genes effectively ameliorates muscular dystrophy in mdx mouse model. Proc Natl Acad Sci USA 2000;97:13714–13719.
15 Wang B, Li J, Fu FH et al. Systemic human minidystrophin gene transfer improves functions and life span of dystrophin and dystrophin/utrophin-deficient mice. J Orthop Res 2009;27: 421–426.
16 Gregorevic P, Blankinship MJ, Allen JM et al. Systemic microdystrophin gene delivery improves skeletal muscle structure and function in old dystrophic mdx mice. Mol Ther 2008;16:657–664.
17 Mendell JR, Rodino-Klapac LR, Malik V. Molecular therapeutic strategies targeting Duchenne muscular dystrophy. J Child Neurol 2010;25:1145–1148.
18 Kole R, Krieg AM. Exon skipping therapy for Duchenne muscular dystrophy. Adv Drug Deliv Rev 2015;87:104–107.
19 Cirak S, Arechavala-Gomeza V, Guglieri M et al. Exon skipping and dystrophin restoration in patients with Duchenne muscular dystrophy after systemic phosphorodiamidate morpholino oligomer treatment: An open-label, phase 2, dose-escalation study. Lancet 2011;378:595–605.
20 Goyenvalle A, Vulin A, Fougerousse F et al. Rescue of dystrophic muscle through U7 snRNA-mediated exon skipping. Science 2004;306:1796–1799.
21 Goyenvalle A, Babbs A, Wright J et al. Rescue of severely affected dystrophin/utrophin-deficient mice through scAAV-U7snRNA-mediated exon skipping. Hum Mol Genet 2012;21:2559–2571.
22 Helderman-van den Enden AT, Straathof CS, Aartsma-Rus A et al. Becker muscular dystrophy patients with deletions around exon 51: A promising outlook for exon skipping therapy in Duchenne patients. Neuromusc Disord 2010; 20:251–254.
23 Long C, Amoasii L, Mireault AA et al. Postnatal genome editing partially restores dystrophin expression in a mouse model of muscular dystrophy. Science 2016;351:400–403.
24 Nelson CE, Hakim CH, Ousterout DG et al. In vivo genome editing improves muscle function in a mouse model of Duchenne muscular dystrophy. Science 2016;351:403–407.
25 Bengtsson NE, Hall JK, Odom GL et al. Muscle-specific CRISPR/Cas9 dystrophin gene editing ameliorates pathophysiology in a mouse model for Duchenne muscular dystrophy. Nat Commun 2017;8:14454.
26 Dumont NA, Wang YX, von Maltzahn J et al. Dystrophin expression in muscle stem cells regulates their polarity and asymmetric division. Nat Med 2015;21:1455–1463.
27 Chang NC, Sincennes MC, Chevalier FP et al. The dystrophin glycoprotein complex regulates the epigenetic activation of muscle stem cell commitment. Cell Stem Cell 2018; 22:755.e6–768.e6.
28 Sacco A, Mourkioti F, Tran R et al. Short telomeres and stem cell exhaustion model Duchenne muscular dystrophy in mdx/mTR mice. Cell 2010;143:1059–1071.
29 Mu X, Usas A, Tang Y et al. RhoA mediates defective stem cell function and heterotopic ossification in dystrophic muscle of mice. FASEB J 2013;27:3619–3631.
30 Lu A, Poddar M, Tang Y et al. Rapid depletion of muscle progenitor cells in dystrophic mdx/utrophin−/− mice. Hum Mol Genet 2014;23:4786–4800.
31 Lim JH, Kim DY, Bang MS. Effects of exercise and steroid on skeletal muscle apoptosis in the mdx mouse. Muscle Nerve 2004; 30:456–462.
32 Tidball JG, Albrecht DE, Lokensgard BE et al. Apoptosis precedes necrosis of dystrophin-deficient muscle. J Cell Sci 1995;108:2197–2204.
33 Higuchi M, Honda T, Proske RJ et al. Regulation of reactive oxygen species-induced apoptosis and necrosis by caspase 3-like proteases. Oncogene 1998;17:2753–2760.
34 Eguchi Y, Shimizu S, Tsujimoto Y. Intracellular ATP levels determine cell death fate by apoptosis or necrosis. Cancer Res 1997;57: 1835–1840.
35 Bonfoco E, Krainc D, Ankarcrona M et al. Apoptosis and necrosis: Two distinct events induced, respectively, by mild and intense insults with N-methyl-D-aspartate or nitric oxide/superoxide in cortical cell cultures. Proc Natl Acad Sci USA 1995;92:7162–7166.
36 Le Moal E, Pialoux V, Juban G et al. Redox control of skeletal muscle regeneration. Antioxid Redox Signal 2017;27:276–310.
37 McCarter GC, Steinhardt RA. Increased activity of calcium leak channels caused by proteolysis near sarcolemmal ruptures. J Membr Biol 2000;176:169–174.
38 Fong PY, Turner PR, Denetclaw WF et al. Increased activity of calcium leak channels in myotubes of Duchenne human and mdx mouse origin. Science 1990;250:673–676.
39 Ng R, Metzger JM, Claflin DR et al. Poloxamer 188 reduces the contraction-induced force decline in lumbrical muscles from mdx mice. Am J Physiol Cell Physiol 2008;295: C146–C150.
40 Wrogemann K, Pena SD. Mitochondrial calcium overload: A general mechanism for cell-necrosis in muscle diseases. Lancet 1976; 1:672–674.
41 Millay DP, Sargent MA, Osinska H et al. Genetic and pharmacologic inhibition of mitochondrial-dependent necrosis attenuates muscular dystrophy. Nat Med 2008;14:442–447.
42 Percival JM, Siegel MP, Knowels G et al. Defects in mitochondrial localization and ATP synthesis in the mdx mouse model of Duchenne muscular dystrophy are not alleviated by PDE5 inhibition. Hum Mol Genet 2013;22:153–167.
43 Reutenauer J, Dorchies OM, Patthey-Vuadens O et al. Investigation of Debio 025, a cyclophilin inhibitor, in the dystrophic mdx mouse, a model for Duchenne muscular dystrophy. Br J Pharmacol 2008;155:574–584.
44 Ascah A, Khairallah M, Daussin F et al. Stress-induced opening of the permeability transition pore in the dystrophin-deficient heart is attenuated by acute treatment with sildenafil. Am J Physiol Heart Circ Physiol 2011;300:H144–H153.
45 Onopiuk M, Brutkowski W, Wierzbicka K et al. Mutation in dystrophin-encoding gene affects energy metabolism in mouse myoblasts. Biochem Biophys Res Commun 2009; 386:463–466.
46 Vila MC, Rayavarapu S, Hogarth MW et al. Mitochondria mediate cell membrane repair and contribute to Duchenne muscular dystrophy. Cell Death Differ 2017;24:330–342.
47 Pant M, Sopariwala DH, Bal NC et al. Metabolic dysfunction and altered mitochondrial dynamics in the utrophin-dystrophin deficient mouse model of duchenne muscular dystrophy. PLoS One 2015;10:e0123875.
48 Sperl W, Skladal D, Gnaiger E et al. High resolution respirometry of permeabilized skeletal muscle fibers in the diagnosis of neuromuscular disorders. Mol Cell Biochem 1997; 174:71–78.
49 Zhang Y, Long C, Li H et al. CRISPR-Cpf1 correction of muscular dystrophy mutations in human cardiomyocytes and mice. Sci Adv 2017;3:e1602814.
50 Handschin C, Kobayashi YM, Chin S et al. PGC-1alpha regulates the neuromuscular junction program and ameliorates Duchenne muscular dystrophy. Genes Dev 2007;21:770–783.
51 Selsby JT, Morine KJ, Pendrak K et al. Rescue of dystrophic skeletal muscle by PGC-1alpha involves a fast to slow fiber type shift in the mdx mouse. PLoS One 2012;7:e30063.
52 Buyse GM, Goemans N, van den Hauwe M, Thijs D, de Groot IJ, Schara U, Ceulemans B, Meier T, Mertens L. Idebenone as a novel, therapeutic approach for Duchenne muscular dystrophy: Results from a 12 month, double-blind, randomized placebo-controlled trial. Neuromusc Disord 2011;21:396–405
53 Qu-Petersen Z, Deasy B, Jankowski R et al. Identification of a novel population of muscle stem cells in mice: Potential for muscle regeneration. J Cell Biol 2002;157:851–864.
54 Gharaibeh B, Lu A, Tebbets J et al. Isolation of a slowly adhering cell fraction containing stem cells from murine skeletal muscle by the preplate technique. Nat Protoc 2008;3:1501–1509.
55 Matre P, Velez J, Jacamo R et al. Inhibiting glutaminase in acute myeloid leukemia: Metabolic dependency of selected AML subtypes. Oncotarget 2016;7:79722–79735.
56 Gao X, Usas A, Lu A et al. Cyclooxygenase-2 deficiency impairs muscle-derived stem cell-mediated bone regeneration via cellular autonomous and non-autonomous mechanisms. Hum Mol Genet 2016;25:3216–3231.
57 Kee PH, Danila D. CT imaging of myocardial scar burden with CNA35-conjugated gold nanoparticles. Nanomed Nanotechnol Biol Med 2018;14:1941–1947.

58 Pisciotta A, Riccio M, Carnevale G et al. Stem cells isolated from human dental pulp and amniotic fluid improve skeletal muscle histopathology in mdx/SCID mice. Stem Cell Res Ther 2015;6:156.
59 Chong J, Xia J. MetaboAnalystR: An R package for flexible and reproducible analysis of metabolomics data. Bioinformatics 2018; 34:4313–4314.
60 Deasy BM, Gharaibeh BM, Pollett JB et al. Long-term self-renewal of postnatal muscle-derived stem cells. Mol Biol Cell 2005; 16:3323–3333.
61 Usas A, Huard J. Muscle-derived stem cells for tissue engineering and regenerative therapy. Biomaterials 2007;28:5401–5406.
62 Lavasani M, Robinson AR, Lu A et al. Muscle-derived stem/progenitor cell dysfunction limits healthspan and lifespan in a murine progeria model. Nat Commun 2012;3:608.
63 Zheng B, Li G, Chen WC et al. Human myogenic endothelial cells exhibit chondrogenic and osteogenic potentials at the clonal level. J Orthop Res 2013;31:1089–1095.
64 Lavasani M, Thompson SD, Pollett JB et al. Human muscle-derived stem/progenitor cells promote functional murine peripheral nerve regeneration. J Clin Invest 2014;124: 1745–1756.
65 Corsi KA, Pollett JB, Phillippi JA et al. Osteogenic potential of postnatal skeletal muscle-derived stem cells is influenced by donor sex. J Bone Miner Res 2007;22:1592–1602.


See www.StemCells.com for supporting information available online.